

BIOMEDICAL SCIENCES INSTRUMENTATION • VOLUME 9

**PROCEEDINGS OF THE
NINTH ANNUAL ROCKY MOUNTAIN BIOENGINEERING SYMPOSIUM
AND TENTH INTERNATIONAL ISA BIOMEDICAL
SCIENCES INSTRUMENTATION SYMPOSIUM**

MAY 1-3, 1972



**PROGRAMMED BY:
RMBS—ISA—IEEE**

BIOMEDICAL SCIENCES INSTRUMENTATION

Volume 9

**Proceedings of the Ninth Annual
Rocky Mountain Bioengineering Symposium
and the
Tenth International ISA
Biomedical Sciences Instrumentation Symposium
held
May 1-3, 1972, Omaha, Nebraska**

Edited By
G. G. Myers
University of Nebraska

**INSTRUMENT SOCIETY OF AMERICA
Pittsburgh, Pennsylvania**

FOREWORD

The papers included in this conference record represent research accomplishments by investigators with a dedicated interest in engineering and the life sciences. Two areas, instrumentation and health care systems, emerged with greatest propensity even though the response to the call for papers covered a very broad spectrum. Neither of these areas could optimally benefit mankind without the other. Hence this emergence reflects the realistic interests of the authors toward a common goal. The papers represent the most current information on bioengineering research available today.

The Ninth Annual Rocky Mountain Bioengineering Symposium and the Tenth International ISA Biomedical Sciences Instrumentation Symposium was sponsored by the Biomedical Sciences Division of the Instrument Society of America; Region Council 4 of the Group on Engineering in Medicine and Biology of the Institute of Electrical and Electronic Engineers, and the Rocky Mountain Bioengineering Symposium, Inc. The Rocky Mountain Bioengineering Symposium is a group of engineers, scientists, and educators of the Rocky Mountain area who sponsor a series of symposia to further the exchange of information on bioengineering. A key feature of these symposia has been the informality of exchange ranging from tutorial papers to current research presentations to evening workshops.

The University of Nebraska has been represented on the Board of Directors of the Rocky Mountain Bioengineering Symposium for a number of years during which bioengineering has experienced real growth and development. The previous eight symposia were held in the Rocky Mountain area. However, the Board of Directors recognized the need to further the exchange of information on a broader geographic scale and it is for this purpose that this year's symposium is being held at the University of Nebraska Medical Center in Omaha. It is with distinct pleasure that I welcome all participants to the symposium and hope that your stay in Omaha is both stimulating and rewarding.

The program is due to the efforts of a number of dedicated people. First I would like to acknowledge the effort of Dr. R. J. Gowen, President of Rocky Mountain Bioengineering Symposium, Inc. Also, the effort of the Program Committee in reviewing the papers and making arrangements was invaluable. The assistance and suggestions by E. C. Lowenberg, R. J. Morgan, J. E. Steadman, F. M. Long, T. W. Nielson, D. Carlson, D. B. Haack, J. Hootman and K. C. Rock, were a major contribution. Also, the supporting effort made possible by R. R. Moutrie, J. P. Gilmore and J. E. Lagerstrom was invaluable in a number of areas.

We are most pleased to be your host and invite you to visit our campus and discuss areas of interest with our students and faculty.

Grant G. Myers, Ph.D.
Program Chairman

CONTENTS

INSTRUMENTATION

DESIGN CONSIDERATIONS FOR THE USE OF FINE AND ULTRAFINE DEPTH BRAIN ELECTRODES IN MAN, A. M. Dymond, T. L. Babb, L. E. Kaechele and P. H. Crandall	1
IMPLANTABLE TRANSDUCER FOR IN VIVO MEASUREMENT OF BONE STRAIN, J. Mallon and D. Germanton	7
A VERSATILE AND ECONOMICAL IMPEDANCE PLETHYSMOGRAPH, L. R. Moffitt	15
A HIGH PERFORMANCE MINIATURE MASS SPECTROMETER FOR RESPIRATORY GAS ANALYSIS, I. E. Sodal, L. Hoivik, A. J. Micco and J. V. Weil	21
CONTROL OF UPPER EXTREMITY ORTHOTIC DEVICES, M. L. Moe, J. T. Schwartz	25

COMPUTER ANALYSIS OF BIOLOGICAL DATA

COMPUTER DETECTION OF DIGITALIS TOXICITY, A. J. Berni, M. W. Lutiges and D. E. Dick	29
DIGITAL TRANSMISSION OF PHYSIOLOGICAL DATA, C. Hyde and D. Bell	33
AN AUTOMATIC FOCUSING ALGORITHM FOR USE IN THE TRACKING OF THREE DIMENSIONAL MICROSCOPE SPECIMENS, D. F. Wann and H. R. Grodsky	37

CARDIOVASCULAR SYSTEM

ORIGIN OF THE DICROTIC NOTCH AND WAVE, R. R. Wemple	45
EFFICACY OF A SMALL, SOLID-STATE DEFIBRILLATOR EMPLOYING TRUNCATED EXPONENTIAL DISCHARGES, W. K. Hagan	49
AN INSTRUMENTATION SYSTEM FOR USE IN ARTIFICIAL HEART RESEARCH, D. R. Carroll, C. S. Swift, M. P. Crawford, P. T. Pearson and N. R. Cholvin	53

HEALTH CARE SYSTEMS

ENGINEERING INVOLVEMENT IN THE DESIGN OF PRIMARY HEALTH CARE DELIVERY SYSTEMS, AN EXAMPLE, G. E. Adams, O. W. Miller, E. M. Simmons and W. P. Sights	59
AN APPROACH TO THE DESIGN OF AMBULATORY HEALTH CARE FACILITIES, C. W. Einolf, Jr., R. A. Perez, J. L. Spicher and J. M. Evans	69
AUTOMATED AND COMPUTERIZED ELECTROCARDIOGRAPHIC SYSTEMS, R. A. Stratbucker	73
A COMPUTERIZED OBSTETRIC INFORMATION SYSTEM, C. C. McCarl and D. C. Amoss	77
COMPUTERIZED GOAL ORIENTED TREATMENT EVALUATION, D. Ramm and D. T. Gianturco	83

MODELS OF PHYSIOLOGICAL SYSTEMS

CARDIOVASCULAR PARAMETER ESTIMATION, J. C. Dennison, D. E. Dick and J. H. Christian	89
MODELING MUSCLE ACTIVATION UNDER NORMAL PHYSIOLOGICAL CONDITIONS, R. E. Hileman	95
A MODEL OF BODY WATER AND SALT REGULATION, F. Badke	103

NEURAL SYSTEMS

ELECTRONIC MODEL FOR NEURAL NETWORKS, R. M. Oliver, R. J. MacGregor and D. A. Leffingwell	109
THE ROLE OF PHOSPHATIDYL SERINE IN NEURAL EXCITATION AND CONDUCTION, E. Low and A. M. Cook	115

CARDIOVASCULAR HEMO-DYNAMICS

A COMPARISON OF VELOCITY PROFILES MEASURED IN UNEXPOSED AND EXPOSED ARTERIES, M. B. Hirst and C. W. Miller	121
FLOW IN A CONSTRICTED TUBE AT A LOW REYNOLDS NUMBER, T. A. Kozman and J. H. Forrester	125
THE EFFECT OF ARTERIAL LOCATION UPON ARTERIAL VELOCITY DISTRIBUTIONS, C. W. Miller, R. C. Nealeigh and M. B. Hirst	129

TELEMETRY

A COMPLETELY IMPLANTABLE THREE CHANNEL TEMPERATURE BIOTELEMETRY SYSTEM, J. R. Decker and M. F. Gillis	133
NON-CONTACT SENSING OF ELECTRIC FIELDS SURROUNDING TROUT, E. M. Lonsdale and W. C. Marshall, Jr.	139
IMPLANT TELEMETRY AND SOCIAL STRAIN, R. D. Rader, C. M. Stevens, J. P. Meehan and J. P. Henry	144

SIGNAL ANALYSIS AND PATTERN RECOGNITION

COMPARISON OF MEDICAL DATA WITH THE EEG IN MATURE ADULTS, S. Halliburton, G. V. Lago and R. S. Daniel	151
STUDIES IN BRAIN PROGRAMED STIMULATION OF THE BRAIN, C. C. Turbes, D. L. Jobe, G. T. Schneider and R. J. Morgan	155
A HYBRID COMPUTER SYSTEM FOR UNSUPERVISED SCORING OF SLEEP RECORDS, P. Courtney and D. Noton	161
MEASUREMENT OF COCHLEAR MICROPHONICS WITH SURFACE ELECTRODES, A. W. Winfield and R. J. Morgan	169

WILDLIFE MANAGEMENT ENGINEERING AND ELECTROMAGNETIC FIELD EFFECTS

BIOTELEMETRY APPLIED TO ELK MANAGEMENT, R. R. Knight, L. S. McLean and G. R. McNeill	171
A TELEMETRY SYSTEM FOR STUDYING ELK BEHAVIOR IN THE ROCKY MOUNTAINS, R. W. Weeks, A. L. Ward and J. Cupal	177
INFLUENCE OF LOW-LEVEL ELECTRIC AND MAGNETIC FIELDS IN THE GROWTH OF YOUNG CHICKENS, W. F. Krueger, J. W. Bradley, A. J. Giarola and S. R. Daruvalla . . .	183
AN ANALYSIS OF HEAT RECEPTORS BY MEANS OF MICROWAVE RADIATION, J. F. Harris and R. I. Gamow	187

APPENDIX	191
AUTHOR INDEX	192
ACKNOWLEDGMENTS	194

DESIGN CONSIDERATIONS FOR THE USE OF FINE AND ULTRAFINE
DEPTH BRAIN ELECTRODES IN MAN

Anthony M. Dymond Thomas L. Babb
Division of Neurosurgery Division of Neurosurgery
UCLA UCLA
Los Angeles, California Los Angeles, California

Lloyd E. Kaechele Paul H. Crandall
Division of Neurosurgery Division of Neurosurgery
UCLA UCLA
Los Angeles, California Los Angeles, California

ABSTRACT

This report summarizes the initial engineering structures of the use of fine electrodes in the human stereotaxic system. Among the factors considered have been the mechanical characteristics of potential electrode materials, electrical recording characteristics, and localization of electrodes placed in the brain. Also considered have been electrode handling and insertion techniques.

The electrode presently under investigation is a coaxial composite of concentric layers of high elastic modulus metal and dielectric, with an overall diameter of about 0.005 inches.

INTRODUCTION

The clinical use of implanted depth brain electrodes in man is constantly increasing, but there has been little change in the types of gross recording electrodes used. These generally consist of a group of wires held together by epoxylite or a similar material. Since it is often desirable to place a number of electrodes into a given region in the brain, smaller electrodes would significantly reduce trauma during implantation. Increased electrode flexibility would also reduce trauma resulting from the small movements of the brain around electrodes fixed rigidly to the skull.

Other practical considerations are related to the implantation technique. In one of the most commonly used systems (1), the individual electrodes are guided to pre-determined targets in the brain through hollow guide screws mounted in the skull. The guide screws are placed by means of a stereotaxic apparatus, using X-rays of the skull and ventricles for reference. Passing the electrodes from outside the head through the screw guides into the brain, presents a pathway through which infection can enter the brain. In addition, the screw guides project out past the scalp and must be protected from external mechanical forces.

This report describes a preliminary investigation of new materials and techniques for producing fine, flexible depth electrodes, and also

implantation techniques for use in the operating room. The design of this system has dealt with the question of electrode materials, handling and insertion techniques, and localization of the implanted electrodes in the brain.

MATERIALS

The relevant mechanical properties of materials considered for electrodes are stiffness and strength. The overall stiffness and strength of an electrode depends on the basic properties of the electrode materials, and the size, shape, and arrangement of materials in the electrode. The basic material property determining stiffness is the modulus of elasticity or Young's modulus, which determines the amount of electrode deflection produced by transverse forces, and the resistance to buckling or bowing produced by axial compressive forces.

Strength is a more complicated property, and can be greatly affected by alloying or by thermal or mechanical processing. The concept of strength requires careful definition. Generally, for electrodes, the strength behavior of interest concerns either breaking (fracture) or else the development of a bend or set in the electrode that does not straighten out when loads are removed (inelastic behavior). For conventional metal electrodes, the latter form of failure is the one of interest. The material property that determines this failure is called the yield stress, and is defined as the load per unit area at which permanent deformation occurs. Below this load, the material springs back to its original configuration when the load is removed. Since yield stress is greatly affected by mechanical and thermal treatment and alloying, it cannot be listed in a definitive fashion as can the elastic modulus. As a general rule, higher modulus materials provide higher yield stresses.

Some materials do break suddenly, with little or no possibility of permanent deformation. In the case of electrodes, these would usually be non-metals such as glass or ceramics. This type of failure is called "brittle" and the related material property is called the fracture stress, expressed as the load per unit area at which this failure occurs. This property is strongly affected

by surface conditions, and is reduced by nicks and scratches on the surface. These materials frequently have high values of elastic modulus, and it is possible to produce nonmetallic electrodes with strengths much higher than with metals. However, this advantage is offset by the undesirable mode of failure, the sudden brittle fracture, that typifies these materials.

Overall electrode strength characteristics are determined by geometry as well as basic material properties. The primary force applied to an electrode during insertion is an axial load to push it in, but some lateral loads may also be imposed. In addition, a variety of force distributions may be applied during fabrication and handling.

Axial forces above a certain level will cause an electrode to buckle, or bow out laterally. The amount of force that can be applied without buckling depends on the size and shape of the cross section of the electrode and also its length. For a round cross section, this load varies with the fourth power of the diameter. This is a powerful effect, and, since the modulus of elasticity has only a linear effect on the buckling load, it follows that materials with low moduli can be used in only slightly larger sizes to compete with the higher modulus materials. However, when attempting to attain the lowest possible electrode sizes, the high modulus materials will always have the advantage.

The unsupported length of the electrode also affects the buckling load, the dependence being with the inverse square of length. For long fine electrodes it may be necessary to devise an insertion technique that reduces the unsupported length.

Considering all the material properties and design factors discussed above, our present thinking favors a coaxial electrode composed of concentric layers of high modulus metal and ceramic. The basic structural core is metal rather than ceramic because of the desirable failure mode if overloaded. This core, also the center electrode, is insulated from the coaxial electrode by a thin dielectric coat. Present plans are based on a ceramic film, either silica or alumina, probably utilizing an advanced coating technology such as sputtering. The coaxial conductor surrounding the dielectric layer is a thin film of gold or platinum, insulated in turn by another coating of ceramic. The selection of core material must satisfy biological compatibility and electrical requirements (2), in addition to providing the desired structural properties. Candidates at this point are tungsten, rhenium, and high iridium alloys of platinum. These all have high elastic moduli, have excellent X-ray absorptivity, and can be obtained in work hardened states with high yield strengths.

Work on prototypes is in progress to determine the mechanical properties of the composite, including the adherence of the coatings when subjected to handling and insertion loads and the integrity of

both the insulating and conducting coatings following these loadings.

HANDLING AND IMPLANTATION OF ELECTRODES

To be of practical use, electrodes must be able to withstand normal handling during fabrication and during use in the operating room. The electrodes must also permit accurate insertion into a target in the brain. For the present application, anatomical and neurosurgical considerations lead to a maximum allowable displacement of an electrode tip of 2.0 mm after transversing 6.0 cm of brain tissue.

The accuracy of placement by hand insertion was used to estimate a practical lower limit of electrode diameter. The smallest electrode studied was a tungsten-boron composition with a 0.004 inch diameter outer layer of boron surrounding a 0.0005 inch inner tungsten core. Studies of placement accuracy with these electrodes were conducted by passing them through a one inch long guide tube placed outside a piece of fresh steer brain. The electrode had to pass into the tissue and transverse an average of 6.0 cm of tissue before emerging from the other side and coming to rest at a ruled target used to score the tip dispersion. The dura was removed from the brain prior to electrode insertion, but the pia mater was intact at both the entry and exit points. Some of the electrode passes crossed a ventricle whose ependyma was intact. The brain tissue was repositioned for each trial to prevent the electrode from traveling along a previous track.

With no tissue in the path of the electrode, the mean dispersion of a group of electrodes was 0.2 ± 0.1 mm. In brain penetration tests, electrodes with symmetrical tips (sharpened with a high speed carborundum wheel) had a mean dispersion of 0.7 ± 0.1 mm. Electrodes with asymmetrical tips had a dispersion of 1.9 ± 0.1 mm, which clearly shows the importance of a symmetrical tip on fine electrodes for accurate guidance through the tissues. Also, these electrodes could be handled without damage during the placement tests.

For comparison, the mean dispersion of 0.005 inch diameter tungsten wires with symmetrical tips was 0.8 ± 0.1 mm. However, it was difficult to make more than a few passes with these electrodes before they were accidentally bent. This fragility would make an all metal electrode of this diameter impractical for use in the operating room, unless much higher yield strength could be provided.

Although the tungsten-boron electrode amply satisfies the criteria for accuracy of placement, it is unsatisfactory in that it undergoes brittle fracture if bent sufficiently. However, this failure mode can be eliminated without greatly decreasing the elastic modulus by increasing the relative amount of metal in the electrode and by slightly increasing the diameter.

These studies showed a practical lower limit for the diameter of fairly long, hand inserted electrodes

to be near 0.005 inches. A composition electrode appears to be a practical way to obtain the necessary values of elastic modulus and yield strength. To implant electrodes of smaller diameter it is necessary to seek novel insertion techniques. Some of the possibilities are high velocity electrode injection, which would use the inertia of the wire to make up for loss of stiffness, or a magnetic technique which would use magnetic fields to guide or even draw the electrode into the brain. The technical problems associated with any of these techniques are formidable.

The effort needed to develop the techniques to implant long electrodes of less than 0.005 inch diameter does not appear justified at this time. A reduction of only a few more thousandths of an inch would be obtained, while the electrodes of larger diameter, which can be inserted by conventional methods, already satisfy the preliminary engineering goals.

Once the techniques for electrode implantation were established, new equipment was designed to do this in the operating room. The system presently under evaluation is shown in Figure 1. It has the advantages of utilizing most of the techniques and hardware presently used in stereotaxic implantation. Rather than having guidance provided by hollow screws placed in the skull, the electrode is directed by an electrode holder traveling through the stereotaxic drill-insertion guide. After a hole is drilled in the skull, the electrode is assisted into the opening by a hand guide which is removed after the electrode has partially entered the brain. The electrode is inserted the rest of the way until a press fit is made between the top of the electrode and the skull. The lead wires from the electrode are then tunneled beneath the skin to a point where they join with other lead wires and leave the skin to be inserted in a plug. This approach does not represent a major departure from the previous techniques, but removes the external guide screws and minimizes the danger of infection.

ELECTRODE LOCALIZATION

It is essential to accurately localize electrodes in the brain since the electrical recordings are used to determine the advisability of surgical procedures (3). The preferred method for determining the position of an electrode is through the use of x-ray radiographs. In some of these cases, prior electrode location within brain structures is confirmed by examination of surgically removed tissue.

Ideally, with precision stereotaxic equipment and a placement technique having small, known tolerances in positions and angles, the electrode position is determined. However, radiographs would always be desirable not only as confirmation of placement but also as a permanent record. Visibility of electrodes is thus an important factor. Larger electrodes generally present no problems, but with the trend to finer electrodes, the qualities that enhance visibility in radiographs become important.

Geometrical properties of the x-ray and electrode system, such as the relative positions of the x-ray source, electrode, and film, affect visibility. Elements having higher atomic numbers and high density are more opaque to x-rays, with the heavy, high atomic number elements having absorptivities equivalent to iron with only a few percent of the thickness. In general, absorptivity decreases rapidly with increasing x-ray energy, but at certain energies there is a very large increase in absorptivity due to the K absorption edge.

X-rays from the sources found in an operating room cover a range of energies, extending downward from the selected energy. The spectrum may also include peaks at energy levels which are characteristic of the target metal of the x-ray tube, and may also be affected by filters placed in the x-ray beam. These factors complicate the effect of electrode material properties, but it is still possible to conclude that electrodes made of the heavier, high atomic number elements should be more easily seen in x-ray radiographs, and the use of higher energies for making radiographs will enhance fine electrode visibility by utilizing K edge absorption.

Some of the effects discussed above are shown in Figure 2, a radiograph of a cadaver head with wires of several sizes and materials placed on the beam source side of the head. (Electrodes within the head would give a slightly sharper image.) It can be seen that the heavy, high atomic number metals are visible in very small sizes, down to about 0.002 inches by using existing equipment and techniques.

ELECTRICAL RECORDING PROPERTIES

Fine electrodes in the size range proposed present no special problems for recording from the brain if the exposed area of conductor is sufficiently large to provide impedances in the range of conventional macroelectrodes. However, if only the cross-sectional area of the fine wire is exposed, the impedance may be much higher, requiring recording amplifiers with high input impedances. In this case, short leads to the amplifiers should be used to avoid radiated interference or cable movement artifact, and impedance transducing with FET's attached to the electrodes is recommended (4).

The suitability of fine wires for recording EEG is illustrated in Figure 3a, which compares EEG waves recorded from monopolar 0.0025 inch diameter electrodes (top four traces), and from bipolar low impedance macroelectrodes situated less than one millimeter from the fine wires. This recording shows the onset of an experimental epileptic attack induced by cobalt in the right ventral hippocampus of a cat. The slow waves at onset, followed by high frequency waves, and then lower frequency oscillations towards the end of the section are recorded equally well by the fine wire electrodes. Figure 3b shows the waveforms of neuronal discharges recorded with a similar fine wire located in the nucleus ventralis anterior of a cat. The ability to detect individual extracellular discharges, which may be recorded for months after

implantation, is an additional advantage of using fine, flexible electrodes.

SUMMARY

The purpose of these investigations has been to decide on the smallest electrode practical for implantation in man. Such electrodes must permit accurate insertion into targets deep in the brain and must be able to withstand normal handling. Based on considerations of strength and stiffness, the electrode selected is a coaxial composite of concentric layers of high elastic modulus metal and dielectric. The inner core and center conductor is metal to insure a failure mode of inelastic deformation, rather than brittle fracture. This inner core is surrounded in turn by concentric layers of dielectric, metal, and outer dielectric. Placement accuracy and handling tests with composite and single material electrodes suggest an overall electrode diameter of about 0.005 inches is feasible. Electrodes of this size can still be localized in the brain with x-ray radiographs, and they have satisfactory recording properties.

Prototype electrodes are being constructed to evaluate the different materials and fabrication techniques available. A modification of the stereotaxic technique used to implant electrodes is also under evaluation.

ACKNOWLEDGEMENTS

The authors wish to thank Mr. R. Sholes for his assistance with the design work.

This work was supported by a grant from the Ralph Smith Foundation, and by USPHS NS 02808.

REFERENCES

1. Talairach, J., David, M., Tournoux, P. L'exploration chirurgicale stereotaxique du lobe temporal dans l'epilepsie temporale. Reperage anatomique stereotaxique et technique chirurgicale, Masson, Paris, 1958, p. 136.
2. Dymond, A.M., Kaechele, L.E., Jurist, J.M., Crandall, P.H., "Brain tissue reaction to some chronically implanted metals", J. NEUROSURGERY, Vol. 33, 574-580, 1970.
3. Crandall, P.H., Brown, W.J., Brinza, K., "Stereotaxic accuracy in vivo of Talairach method in temporal lobes", CONFIN. NEUROL., Vol. 27, 149-153, 1966.
4. Brackel, S., Babb, T., Mahnke, J., Verzeano, M., "A compact amplifier for extracellular recording", PHYSIOL. BEHAV., Vol. 6, 953-995, 1971.

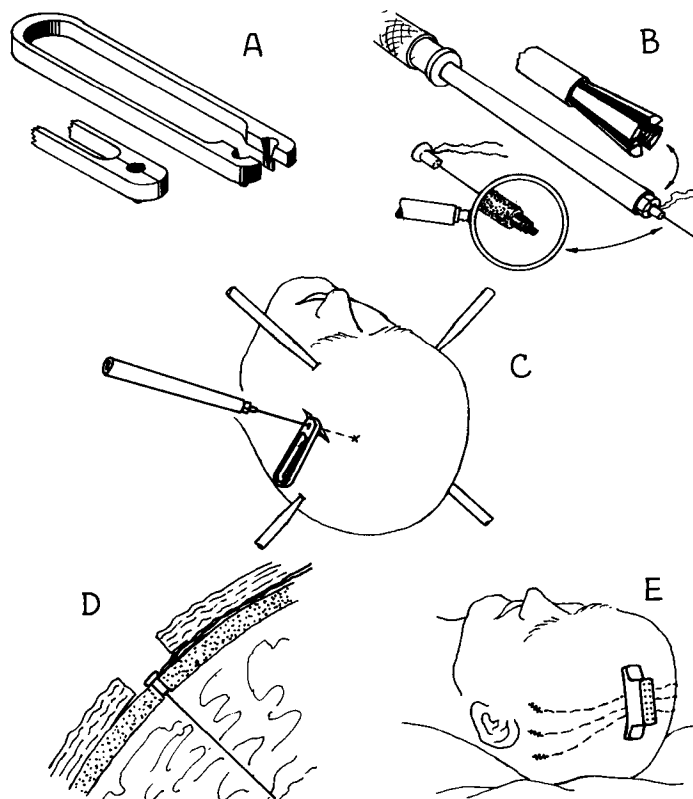


Figure 1: A system under evaluation for implantation of electrodes in man.
A. - Hand guide for assisting an electrode into a skull bur hole.
B. - Stereotactically guided electrode holder loaded with a fine coaxial electrode.
C. - Use of the electrode holder and hand guide to place an electrode into a head mounted in the stereotaxic frame.
D. - Cross-sectioned view of an electrode in place with the lead wires tunneled beneath the skin.
E. - View showing lead wires tunneled to a central connector plug after scalp closure over the electrode entry points.

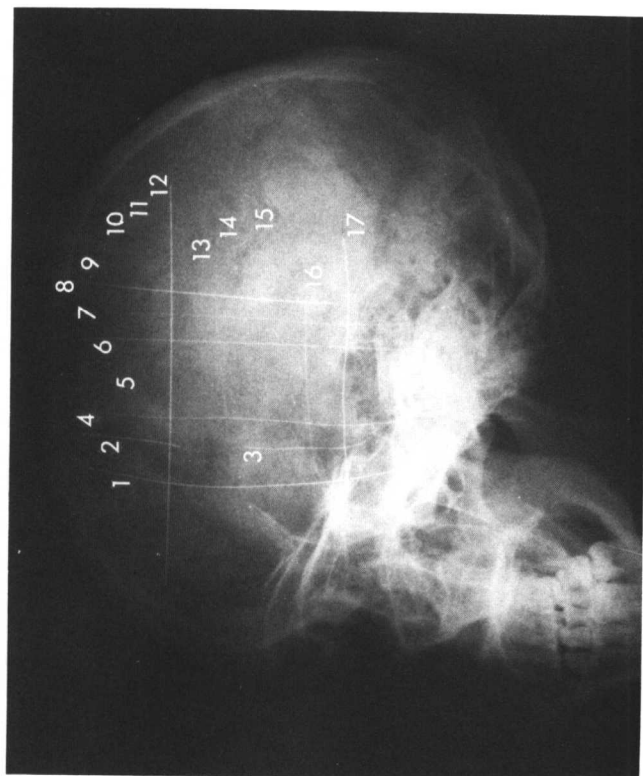


Figure 2 : Radiograph (65 kV, 300 mA.sec) of a cadaver head with wires of several sizes and materials placed on it.

1. - Rhenium, 0.0096 inch diameter.
2. - Platinum-10% Iridium, 0.0065 inch.
3. - Platinum-10% Rhodium, 0.0065 inch.
4. - Rhenium, 0.006 inch.
5. - Tungsten, 0.0005 inch, surrounded by 0.004 inch diameter layer of boron.
6. - Stainless steel tubing, 0.014 inch O.D. and 0.007 inch I.D.
7. - Stainless steel 0.009 inch.
8. - Tungsten, 0.010 inch.
9. - Platinum-15% Rhodium-6% Ruthenium, 0.0016 inch.
10. - Iron 61% Nickel-15% Chromium, 0.0018 inch.
11. - Nickel-20% Chromium, 0.0025 inch.
12. - Steel, 0.202 inch.
13. - Platinum-15% Rhodium-6% Ruthenium, 0.002 inch.
14. - Stainless steel, 0.006 inch.
15. - Platinum-10% Iridium, 0.002 inch.
16. - Five strands of Platinum-15% Rhodium-6% Ruthenium, 0.0016 inch.
17. - Platinum-30% Iridium, 0.008 inch.

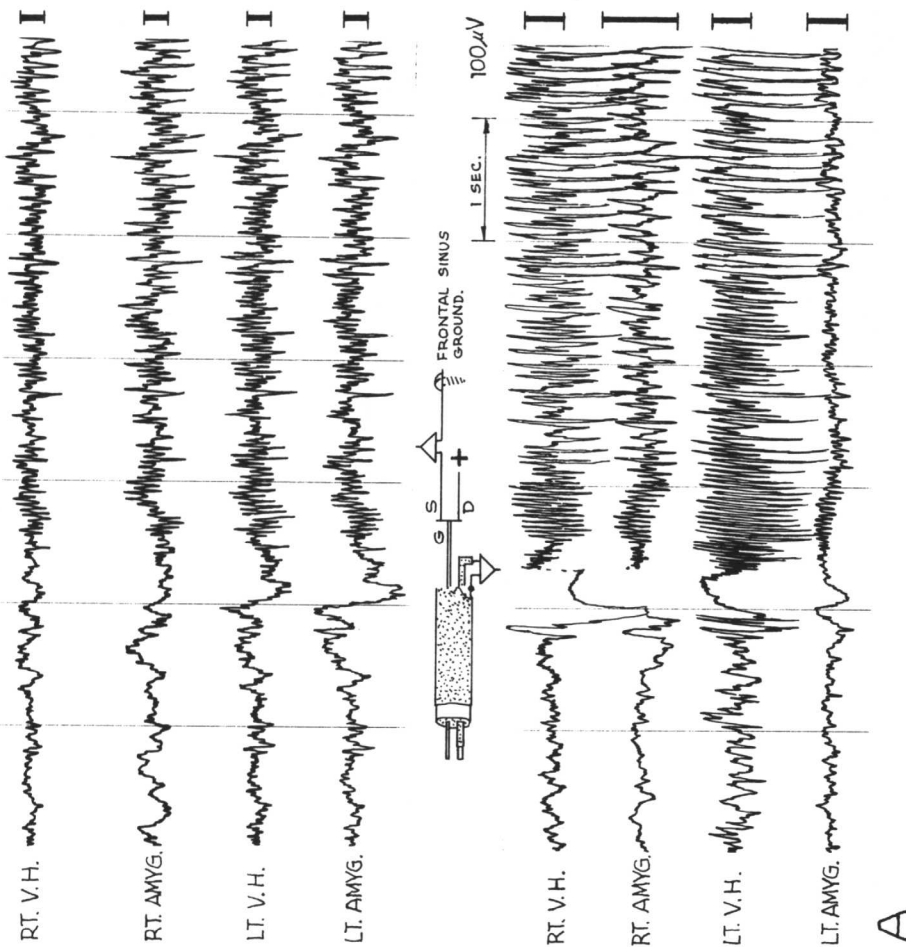


Figure 3:

- A. - Comparison of EEG waves from monopolar 0.0025 inch diameter fine wire electrodes (four top traces), and from bipolar macro-electrodes situated less than one millimeter away from the fine wires (four bottom traces). The relationship between the recording electrodes and amplifiers is shown in the insert. The records show the onset of an experimental epileptic seizure in a cat.
- B. - A pair of extracellular neuronal discharges recorded by a similar fine wire one month after implantation into the thalamus of a cat.

IMPLANTABLE TRANSDUCER FOR IN VIVO
MEASUREMENT OF BONE STRAIN

Joseph Mallon

Damon Germanton

Kulite Semiconductor Products, Inc.
Ridgefield, New Jersey

ABSTRACT

This paper describes the result of a development effort to design and fabricate a strain transducer suitable for implantation in the tibia bone of a rhesus monkey. The transducer described uses a unique monolithic integrated circuit as the sensing element. The design is discussed in detail, and experimental data are presented.

INTRODUCTION

Recently, for a variety of reasons, much attention has been focused in the area of adapting technologies developed in the aerospace industry to earthbound problems. In particular there is considerable interest in using sophisticated data acquisition and analysis techniques to obtain quantitative data on biological parameters in research, diagnostic and clinical situations. The techniques and hardware developed by the aerospace industry for data analysis have a high degree of generality and can be applied with much success in biomedical settings. The transduction of physical parameters (pressure, force, acceleration, displacement, etc.) in living organisms, however, often presents new technical problems and requires the development of transducers which are problem-specific in their design. This paper discusses the application of a particular solid-state phenomena, semiconductor piezoresistance, to the measurement of a biological parameter, bone strain. The approach makes use of a property observed by solid-state researchers in the mid-fifties,¹ a fabrication technology developed for the production of integrated circuits in the early sixties and bridges the gap between its first large scale use in aerospace and the present biomedical problem.

The problem approached is to design a strain transducer suitable for long-term implantation in the tibia bone of a rhesus monkey.

In order to provide usable output at low strain levels, the use of a semiconductor sensor with its high inherent sensitivity (2 orders of magnitude over conventional metallic strain gages) is dictated.

The fracture strain of bone material² may be as high as 12,000 $\mu\text{in/in}$. Since semiconductor strain gages are limited to strain levels of approximately 4000 $\mu\text{in/in}$, a strain reducing flexure must be incorporated in the design.

One approach is to modify a standard extensometer design to make it suitable for implantation. This approach, however, has several inherent disadvantages. First, extensometers tend to be rather large. Second, and more seriously, an extensometer must be mounted external to the bone. External mounting aggravates the problem of interaction between muscle tissue and the transducer. In order for such a transducer to function properly in vivo, a cover which effectively prevents the ingress of body fluids must be provided, but the mechanical configuration of an extensometer makes design of a suitable cover difficult.

The approach pursued makes use of a cylindrical strain transducer which is sensitive to diametrical compressive and tensile strain. The sensing element is a diffused element semiconductor strain gage mounted internal to the cylinder. The transducer may be potted in place with a suitable medical grade epoxy or it may be force fit into the bone, the latter method being the preferred technique. It is designed for insertion into a one-eighth-inch hole drilled in the test animal's bone as shown in Figure 8.

TRANSDUCER DESIGN

a) Sensor Design

The sensing element is a unique diffused monolithic semiconductor strain gage bridge used as a bending beam. It consists of a thin beam of monocrystalline silicon on which integral piezoresistive elements have been formed by solid-state diffusion of boron. This approach has the advantage that the force collector (bending beam) and the sensors (diffused piezoresistors) are an integral unit as opposed to the conventional technique of cementing the sensors (semiconductor or metallic strain gages) to the force collector. Thus, problems associated with creep, slippage and hysteresis of organic epoxies are avoided.

Gage configuration is determined by using oxide masking and photolithographic techniques allowing the fabrication of very small geometries. The stress sensors are isolated from the beam by the presence of a p-n junction. Details of the design and fabrication of such sensors have been discussed extensively in the literature by Kurtz et al. and will not be repeated here. Ref. 3, 4, 5.

Figure 1 shows the construction of the basic sensing element. The crosshatched areas are p-type regions formed by solid-state diffusion of boron through appropriately shaped windows in a masking layer of thermally grown silicon dioxide. The larger areas to which the leads are affixed are metallized contact lands, while the narrow interconnecting stripes are the piezoresistive elements.

Two longitudinal elements (R_L) and two transverse elements (R_T) are interconnected to form a Wheatstone bridge, as shown in Figure 2. Such a circuit provides inherent temperature compensation since temperature induced resistance changes are the same for all four arms and consequently are nulled out. Variations in the level of bone strain are converted by a mechanical flexure to simple longitudinal bending of the diffused sensor, and for full output from the Wheatstone bridge shown in Figure 2, the gages designated R_T must have a negative resistance change with respect to those designated R_L . This is accomplished by utilizing transverse sensitivity for R_T and longitudinal sensitivity for R_L . The longitudinal piezoresistive coefficient (π_L) is given by,

$$\pi_L = \pi_{11} - 2(\pi_{11} - \pi_{12} - \pi_{44}) \cdot K \quad (1)$$

where K is $(\ell_1^2 m_1^2 + \ell_1^2 n_1^2 + m_1^2 n_1^2)$

ℓ_1, m_1, n_1 are direction cosines of the current direction with respect to the crystallographic directions.

$\pi_{11}, \pi_{12}, \pi_{44}$ are the fundamental piezoresistive coefficients.

The transverse piezoresistive coefficient π_T is given by,

$$\pi_T = \pi_{12} + (\pi_{11} - \pi_{12} - \pi_{44}) \cdot K \quad (2)$$

For p-type silicon of the orientation shown in Figure 2,

$$\pi_L = \frac{1}{2} \pi_{44} \quad (3)$$

$$\pi_T = -\frac{1}{2} \pi_{44} \quad (4)$$

The resistance change under an applied stress is related to the piezoresistive coefficient by,

$$\frac{\Delta R}{R} = \pi \sigma \quad (5)$$

where π may be either π_L or π_T

It can be seen then, for the orientation used, a uniaxial stress σ will produce a negative resistance change in R_T and a positive resistance change of equal magnitude in R_L . The orientation chosen yields maximum values of $\Delta R/R$ under the restraining condition that $\pi_L = -\pi_T$. For the impurity concentration levels used the resistance change at an appropriate full scale stress will be on the order of 3%. The output of a Wheatstone bridge is approximated by,

$$V_o = \frac{\Delta R}{R} V_{in} \quad (6)$$

So full scale output levels on the order of 30 mv/v might be expected.

b) Mechanical Design of Transducer

(1) Force Collecting Element

In order to measure the strain in living bone accurately, the displacement of a fixed point with respect to another must be determined without affecting the displacement by the presence of the measuring device. The effective stiffness of the measuring device must therefore be the same or lower than that of bone. The force collecting element of the transducer is a cylinder in diametric compression. The internal sensing elements of the transducer, as will be shown in a subsequent section, have a negligible effect on the elastic behavior of the cylinder and can thus be neglected in the cylinder

displacement calculations.

The force applied to the cylinder under the maximum strain condition in the tibia of the monkey of 12,000 μ in is given by,

$$F_1 = E_1 \cdot \epsilon_1 \cdot A \quad (7)$$

$$= 120 \text{ lbs.}$$

where F_1 is the total unidirectional force on the cylinder

E_1 is Young's Modulus for bone ($\sim 2 \times 10^6$ psi)

ϵ_1 is the strain in the bone under conditions of maximum loading ($12,000 \times 10^{-6}$ in/in)

A is the projected area on the cylinder in the direction of the force $A = b \cdot d = 5 \times 10^{-3}$ in

The cylinder must have an effective stiffness equal to or lower than that of bone (2×10^6 psi). Assuming that the cylinder follows the bone, the change in diameter is given by,

$$\Delta d = d \epsilon_1 \quad (8)$$

$$= 1.5 \times 10^{-3} \text{ in}$$

where d is the diameter of the transducer (.125")

ϵ_1 is the maximum strain in the bone ($12,000 \times 10^{-6}$ in/in)

The relationship between the parameters of the cylinder and the required force to produce a given deflection is as follows,

$$F_2 = \frac{E b t^3 \Delta d}{1.79 r^3} \quad (9)$$

$$= 25.5 \text{ lbs.}$$

where F is the force required to deflect the cylinder

t is the wall thickness (.016")

r is the radius (.054")

b is the length of the cylinder (.040")

Δd is the change in diameter under maximum strain (.0015")

E is Young's Modulus of the cylinder material (30×10^6 psi for stainless steel)

This calculation applies only to point

forces radially aligned as in Figure 4.

In fact, the force is distributed over the entire surface of the cylinder at a varying angle of application. If this factor is accounted for, it can be shown that the actual force required to deflect the cylinder is twice the calculated force (56 lbs.) As was shown in Equation (7) the force available under the maximum strain condition in the bone is 120 lbs. Thus using the indicated dimensions, approximately twice the force necessary to deflect the cylinder is available. The force required is designed low by a factor of two, in order to preclude the possibility of the cylinder being stiffer than the bone due to tolerance build-up. Provided the force required is less than the force available, the transducer will measure the true deflection. The thin ends of the cylinder are merely for attachment of the end plates. These end plates have been neglected in the calculations because the stiffness varies as the cube of the thickness. The presence of these plates stiffens the transducer by a negligible amount.

(2) Flexure Design

The sensing element shown in Figure 4 is a "U" shaped flexure made up of stainless steel moment arms and the diffused silicon bending beam described previously.

When diffused beam is bent in an arc with the gages on the tension side, the inner gages increase in resistance due to the positive gage factor of the gages in tension, while the resistance of the outer gages decreases due to their negative transverse gage factor.

When a force is applied as indicated in Figure 4, the bending moment and thus the strain will be uniform over the diffused beam. Therefore, the gages can be placed at any location along the axis of the beam without loss in sensitivity. The flexure is designed to provide a 6 to 1 strain reduction ratio, allowing the use of semiconductor strain gages at an appropriate full scale strain level of 2000 μ in/in for a bone and cylinder strain of 12,000 μ in/in. The magnitude of the force required to deflect the U-beam⁶ to full scale is given by,

$$F = \frac{\epsilon_2 E w t}{(1 + \frac{\delta C}{t})} \quad (10)$$

$$= .094 \text{ lb.}$$

where ϵ_2 is the strain in the beam at maximum cylinder deflection (2000×10^{-6} in/in)

w is the width of the beam (.030")

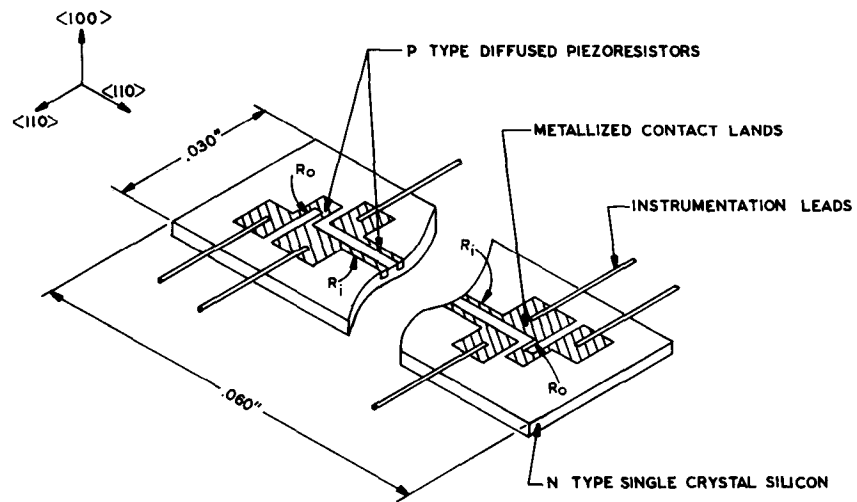


FIGURE 1 MONOLITHIC STRAIN SENSOR UTILIZING BOTH LONGITUDINAL AND TRANSVERSE PIEZORESISTIVITY

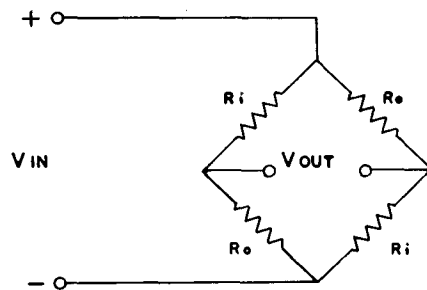


FIGURE 2 FULLY ACTIVE STRAIN SENSITIVE WHEATSTONE BRIDGE

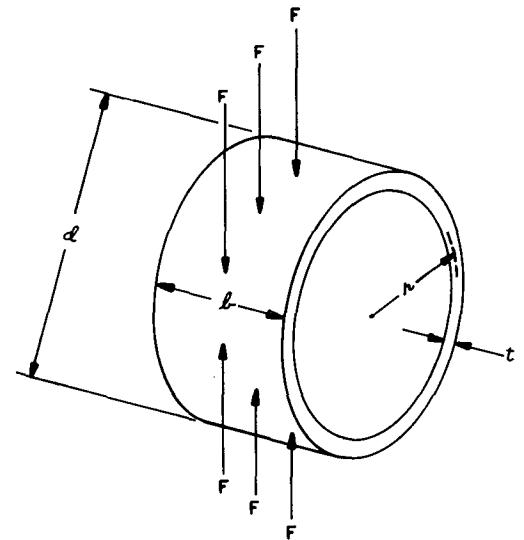


FIGURE 3 FORCE COLLECTING ELEMENT

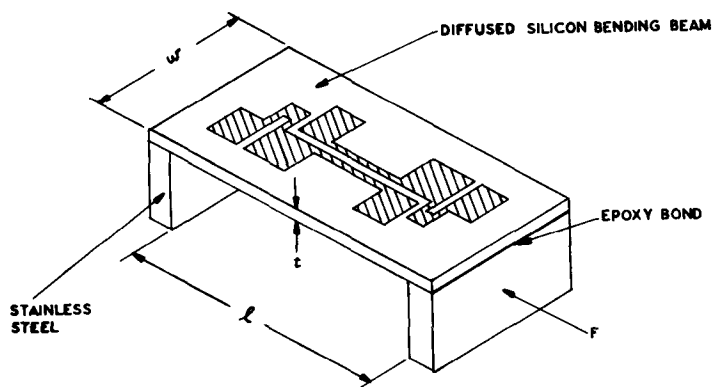


FIGURE 4 FLEXURAL ELEMENT

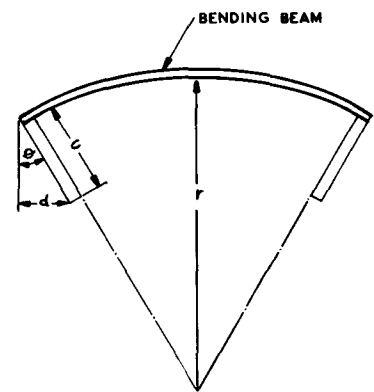


FIGURE 5 U-FLEXURE SHOWN BENT UNDER AN APPLIED LOAD

t is the thickness of the
diffused beam (.0025")

C is the moment arm from the beam
to the applied force (.020")

E is the modulus of elasticity of
silicon (30×10^6 psi)

Thus the force required to bend the internal sensing element is more than three orders of magnitude less than the force required to deflect the cylinder. This justifies the neglect of the effect of the flexural element in cylinder stiffness calculations.

The required beam thickness is determined by applying two geometric relationships (11, 12) for the U-flexure with the condition that the strain in the beam is to be 2000 $\mu\text{in/in}$ at a bone strain of 12,000 μin . When the forces are applied as in Figure 5, the beam describes a circular arc with the moment arms perpendicular to the ends of the beam. The moment arms are thick enough with respect to the beam that it can be assumed that there is no bending in these arms.

It can readily be seen from Figure 5 that the relationship between the deflection (d) and the deflection angle (θ) is,

$$\sin \theta = \frac{d}{C} \quad (11)$$

The second geometric relationship relating the strain (α) to the thickness of the beam is given by,

$$\alpha = \frac{X(1 + \epsilon) - X(1 - \epsilon)}{2} \quad (12)$$

$$\alpha = X\epsilon$$

Since, for small deflections, X is approximately equal to L,

$$\alpha = L\epsilon$$

but by inspection of Figure 5,

$$\sin \theta = \frac{\alpha}{t} \quad (13)$$

therefore,

$$\sin \theta = \frac{L\epsilon}{t} \quad (14)$$

but from Equation (10),

$$\sin \theta = \frac{d}{C}$$

so,

$$\frac{L\epsilon}{t} = \frac{d}{C} \quad (15)$$

$$t = \frac{L\epsilon C}{d}$$

$$t = 2.46 \times 10^{-3} \text{ in}$$

where L is the length of the bending
(46×10^{-3} in)

ϵ is the maximum strain in the
bending beam (2000×10^{-6} in/in)

C is the moment arm from the beam
to the applied force (20×10^{-3} in)

d is one-half the deflection of the
cylinder under maximum strain
(0.75×10^{-3} in)

FABRICATION

The assembly details are shown in Figure 7. The transducer housing is fabricated from body-compatible stainless steel. The end caps are affixed with medical grade RTV adhesive. Tests have shown that the construction techniques used, prevent the ingress of a saline test solution for at least 200 hours at body temperature. The overall tolerance on the o.d. of the transducer is held very closely to allow force fitting into an accurately drilled hole in the bone as shown in Figure 8. Alternately, the transducer may be mounted in a somewhat larger hole and secured with a medical grade epoxy.

EXPERIMENTAL DATA

A number of bone strain transducers were built and tested with good results. Figure 9 is a plot of bridge output vs. strain at an input voltage of 5 volts. The sensitivity is close to the expected value, and, although some nonlinearity is observed, it is deemed acceptable. Variation in sensitivity from unit to unit was found to be approximately 25% and was undoubtedly due to tolerance build-up. Repeated tests showed that the hysteresis and repeatability were excellent.

An important consideration in a transducer designed for in vivo measurements is that the construction be such as to prevent the ingress of body fluids over extended period of time. Accordingly several completed transducers were immersed in a saline solution and held at body temperature for a period of 200 hours. No gross change in the transducer no-load output voltage was observed during this period, indicating that the seals were leak free.

Another important consideration is that the transducer should exhibit no change in its characteristics when used at body temperatures. The monolithic strain sensor employed in the subject transducer possesses inherent self-compensation for variation of zero with temperature. The

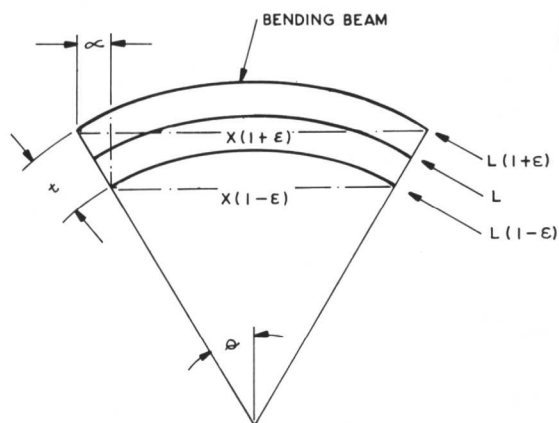


FIGURE 6 CROSSSECTION OF DIFFUSED BEAM SHOWN BENT UNDER AN APPLIED LOAD

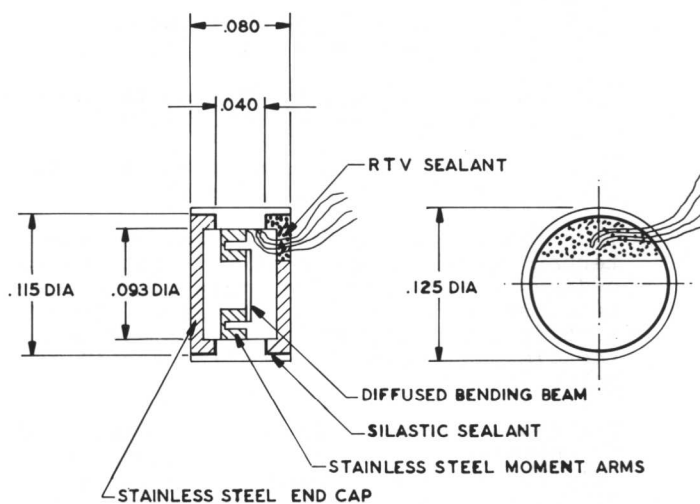


FIGURE 7 ASSEMBLY DRAWING FOR BONE IMPLANTABLE TRANSDUCER

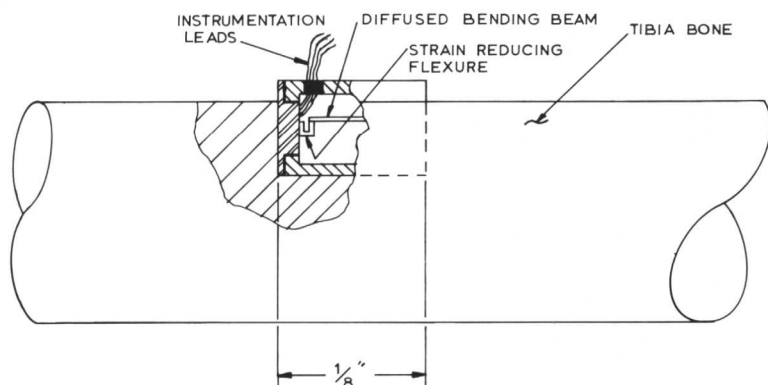


FIGURE 8 DIFFUSED ELEMENT STRAIN TRANSDUCER SHOWN IMPLANTED IN TIBIA BONE OF MONKEY

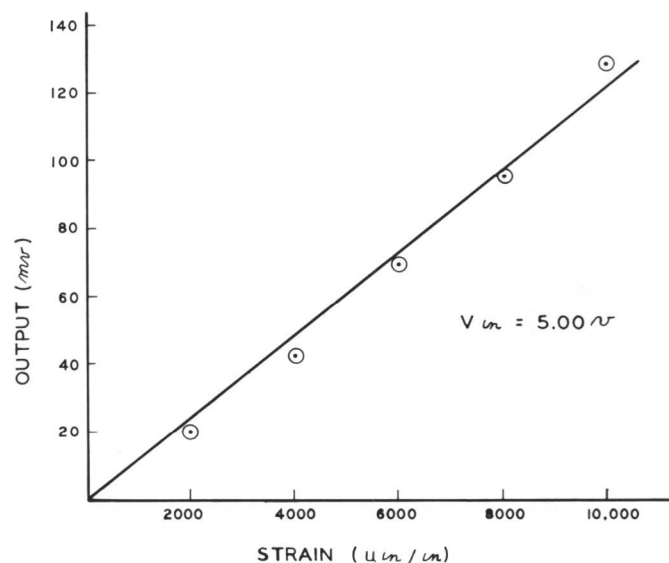


FIGURE 9 TYPICAL CALIBRATION CURVE FOR BONE IMPLANTABLE TRANSDUCER

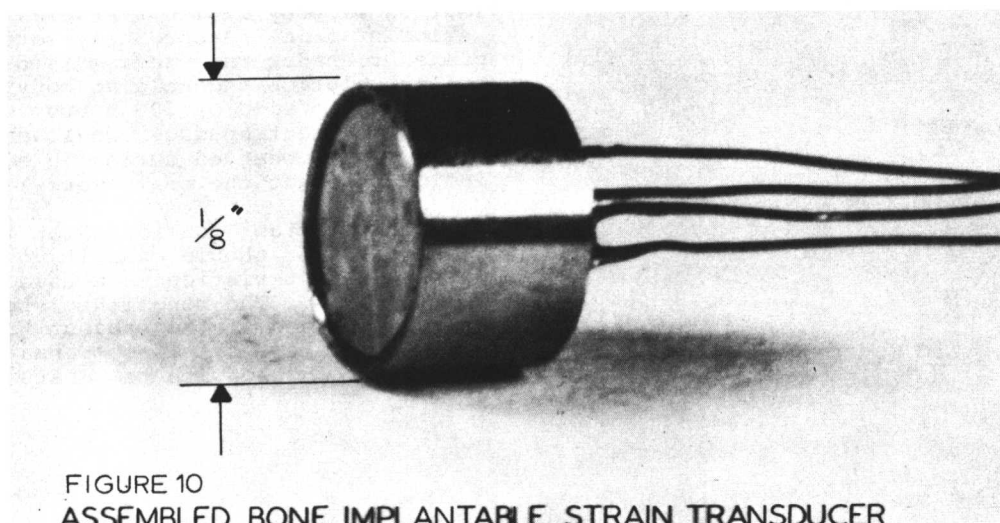


FIGURE 10 ASSEMBLED BONE IMPLANTABLE STRAIN TRANSDUCER